Application of population balance equation for continuous granulation process in spherodizers and rotary drums

Ludmila Vesjolaja[1] Bjørn Glemmestad[2] Bernt Lie[1]

[1]Department of Electrical Engineering, IT and Cybernetics, University of South-Eastern Norway, {ludmila.vesjolaja,bernt.lie}@usn.no
[2]Process Modeling and Control Department, Yara Technology Center, Norway, bjorn.glemmestad@yara.com

Abstract

In this paper, a dynamic model for a granulation process is developed. A population balance is used to capture dynamic particle size distribution in the spherodizer model and in the rotary drum granulator model. Particle growth due to layering is assumed in the spherodizer simulation model, while particle binary agglomeration is taken as the main granulation mechanism in the rotary drum simulation model. The developed models are 2-dimensional(2D) models that are discretized in terms of its internal coordinate (particle diameter), external coordinate (axial length of the granulators). Simulations using the developed models provide valuable data on dynamic fluctuations in the outlet particle size distribution for the granulators. In addition, the simulations results give a valuable information for the control studies of the granulation process. The simulation results showed that the extension of the model from 1D model to 2D model using the discretization of the external coordinate in the model, introduces a transport delay that is important in control studies.

Keywords: spherodizer, rotary drum, population balance, dynamic model, time delay

1 Introduction

Granulation processes are used in a wide range of industrial applications, including fertilizer industries. Fertilizer manufacturing using the granulation process has received considerable research interest during the last few decades, due to (i) the increasing requirements for efficient production of high quality fertilizers for increased food production in a growing global population, and (ii) difficult process control and operation, e.g., among others (Herce et al., 2017; Ramachandran et al., 2009; Valiulis and Simutis, 2009; Wang et al., 2006) and (Cameron et al., 2005) have focused their research on granulation processes. This paper is focused on the last part of the mineral fertilizer production, i.e. on the granulation loop. The granulation loop is used to produce different grades of fertilizers. A typical schematic of a granulation process with the recycle loop is shown in Figure 1. The granulation loop consists of a granulator, granule classifier (screener), and a crusher. The granulator receives the fines from the external particle feed, as well as from the recycled styream. These particle feeds are sprayed with a fertilizer liquid melt (slurry), and granules are formed. Different granulation mechanisms depending on the granulator type and conditions are responsible for these granule formation.

Process control of granulation loops is challenging. Typically, the PSD of the granules leaving the granulator is wider compared to the required PSD of the final product. A typical recycle ratio between the off-spec particles (80 %) and the required product-sized particles (20 %). Thus, it is important to develop a dynamic model that could further be used in control relevant studies. This paper is focused on developing dynamic models of two types of granulators, namely spherodizers and rotary drums. Depending on the granulator type and operating conditions, different granulation mechanisms (granule formation mechanism) are predominant. In spherodizers, the main granulation mechanism is particle growth due to layering. Layering is a continuous process during which particle growth occurs due to a successive coating of a liquid phase onto a granule. In rotary drum granulators, on the other hand, particle collision occurs, and thus particle agglomeration contributes significantly to particle size change. In this paper, binary particle agglomeration is assumed for population balance (PB) modeling. Binary agglomeration refers to a granule formation mechanism that occurs due to successful collision of two particles, resulting in the formation of a larger, composite particle (Litster and Ennis, 2004; Vesjolaja et al., 2018).

This paper is an extension of our previous study that is summarized in (Vesjolaja et al., 2018). Here, the dynamic model of the granulator is improved by increasing the dimensionality of the model, i.e., a 2D model instead of a 1D model is developed. The improved dynamic model provides valuable data on dynamic fluctuations in the outlet particle size distribution for the granulators. Thus, the contributions of this paper are: (i) the 1D model is extended to the 2D model (ii) developed 2D models are applied for two types of granulators, spherodizers and rotary drums, and (iii) two different numerical schemes, a finite volume scheme and a sectional scheme, are applied to the developed 2D dynamic models.

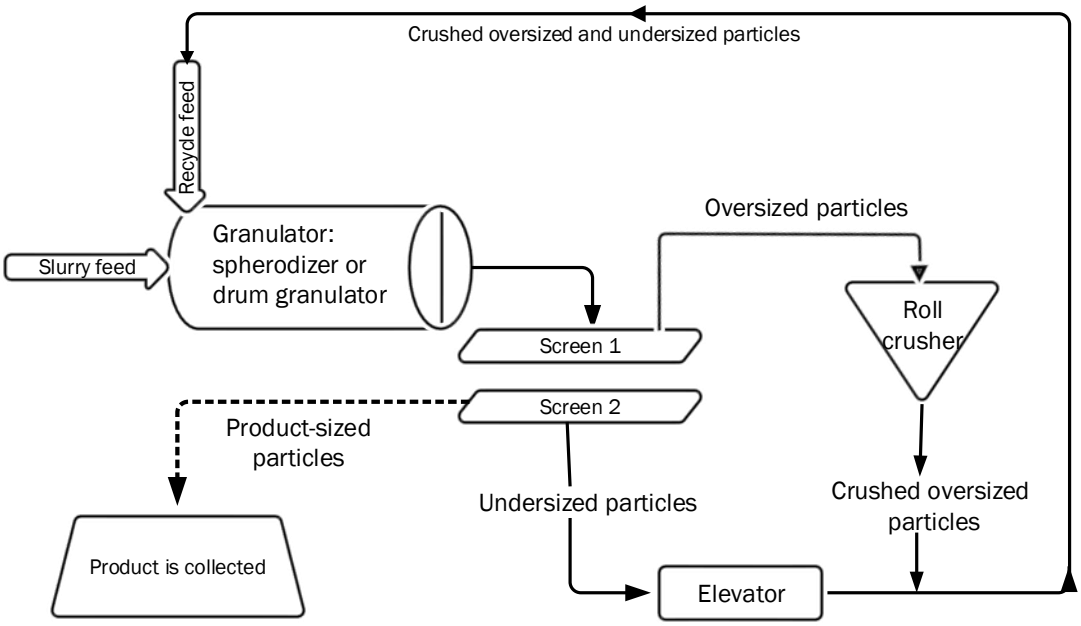

Figure 1. Schematic diagram of granulation loop.

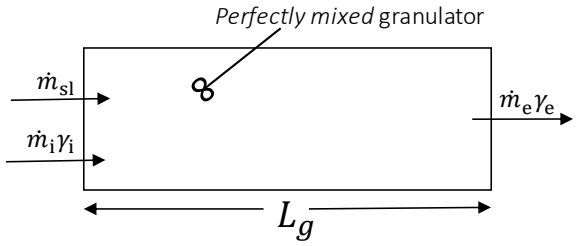

Figure 2. Graphical representation of the *perfectly mixed* granulator.

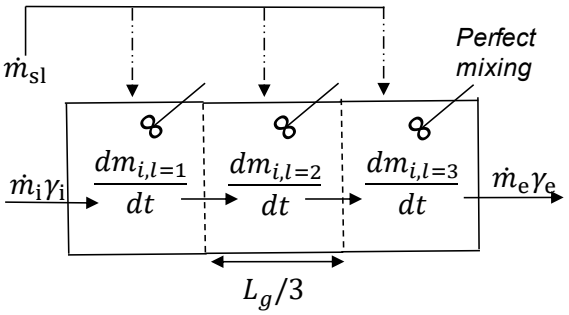

Figure 3. Graphical representation of the multi-compartment granulator. Abreviations: N_z is the number of the compartments in the granulator; L_g is the length of the granulator.

2 Application of PBE to granulation process in spherodizers

In the fertilizer production plant under consideration, a continuous granulation process is used. In an industrial application, it is relatively easier to work with mass based population balance equations (PBEs) instead of number based PBEs due to (i) the PSD in a real plant is typically measured by sieving and weighting, and (ii) mass based PBE is more convenient to use from a numerical point of view due to a huge number of particles compared to their mass. In addition, the size of the particles is represented in terms of their diameters (L) since measuring of PSDs in the plant are based on sieve diameter. A number based PBE with particle volume as internal coordinate is described in (Ramkrishna, 2000). Thus, it is essential to convert PBEs from their volume based formulations to length based formulations. In addition, number based PBEs should be converted into mass based PBEs. The mass based PBE for the spherodizer (continuous layering process) taking particle diameter as the internal coordinate, is formulated as

$$\frac{\partial m(L,z,t)}{\partial t} = -L^3 \frac{\partial}{\partial L}\left[G\frac{m(L,z,t)}{L^3}\right] - \frac{\partial}{\partial z}\left[\frac{dz}{dt}m(L,z,t)\right]. \quad (1)$$

where m is the mass density function $\left[\frac{kg}{mm^3 \cdot [mm}\right]$. The first term on the right hand side represents the particle growth due to layering, while the last term represents a continuous process and gives the flow of particles through the granulator. G is the growth rate $\left[\frac{mm}{s}\right]$. Equation 1 is derived by assuming that all particles are ideal spheres

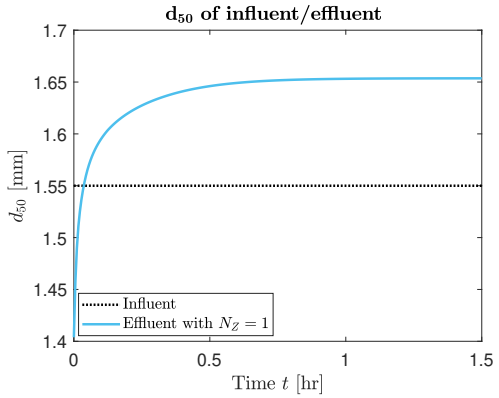

Figure 4. d_{50} for influent and effluent.

with a constant solid density ρ.

Here, the particle growth rate for layering (G) is modeled assuming a linear size-independent growth rate. Mathematical expressions for a linear size-independent growth rate are given in Equation 2.

$$G = \frac{2\dot{m}_{\mathrm{sl}}(1-X_{\mathrm{sl,i}})}{\rho A_{\mathrm{p,tot}}}, \qquad A_{\mathrm{p,tot}} = \pi n \int_{L=0}^{L=\infty} L^2 dL, \tag{2}$$

where $\dot{m}_{\mathrm{sl}}$ is the fresh fertilizer spray rate, $X_{\mathrm{sl,i}}$ is the moisture fraction in the slurry and total $A_{\mathrm{p,tot}}$ is the surface area of the particles.

2.1 Internal coordinate

Integration of Eq. 1 for i-th size class gives

$$\frac{dM_i}{dt} = L_i^3 G \cdot \left[m\left(t, L_{i-\frac{1}{2}}\right) - m\left(t, L_{i+\frac{1}{2}}\right) \right]. \tag{3}$$

For simplicity, in Equation 3, the particle flux term is neglected as it is dependent on the external coordinate (the discretization of the external coordinate is described in Section 2.2).

Discretization of the internal coordinate, i.e., discretization of the growth term for particle diameter, has been performed using a finite volume scheme extended by a flux limiter function. High resolution schemes are considered to attain higher accuracy than the first order upwind schemes. In addition, these methods avoid spurious oscillations by applying a high order flux in the smooth regions and a low order flux near discontinuities (Koren, 1993; Kumar, 2006). In this paper, a Koren flux limiter function (KFL) is used to achieve a robust upwind discretization scheme to Eq. 3. Discretization of the internal coordinate is performed on a linear grid using the KFL scheme. KFL scheme for the mass based PBE with the particle diameter (not volume) as internal coordinate is given in (Vesjolaja et al., 2018).

2.2 External coordinate

For a continuous granulation process, a plug flow along the axial direction is assumed. Here, the external coordinate (particle fluxes in and out of the granulator), given by the term $\frac{\partial}{\partial z}\left[\frac{dz}{dt} m(L,z,t)\right]$ is treated in two different ways as described below as Case I and Case II, respectively.

Case I: In this simplified case, a concept of *output equivalent* inside the granulator is used (Figure 2). This means that the entire granulator is treated as *perfectly mixed* throughout its length (L_{g}). The whole granulator is treated as a single compartment with $N_z = 1$ where N_z denotes the number of compartments. Thus, the particle flux term reduces to

$$\frac{\partial}{\partial z}\left[\frac{dz}{dt} m(L,z,t)\right] = \dot{m}_{\mathrm{i}}\gamma_{\mathrm{i}} - \dot{m}_{\mathrm{e}}\gamma_{\mathrm{e}}, \tag{4}$$

where the particle flux out from the granulator is defined as

$$\dot{m}_{\mathrm{e}}\gamma_{\mathrm{e}} = \frac{m_i}{\tau}\gamma_{\mathrm{e}}. \tag{5}$$

Here, $\dot{m}_{\mathrm{i}}$ is the mass flow rate of particles entering the granulator (influent), $\dot{m}_{\mathrm{e}}$ is the mass flow rate of particles leaving the granulator (effluent), γ_{i} is the size distribution function of the influent, γ_{e} is the size distribution function of the effluent, m_i is the mass of the i-th particle size class, and τ is the retention (residence) time.

Case II: In this case, the granulator is divided into N_z equally sized compartments, Figure 3. The influent to the granulator enters the 1-st compartment and the effluent leaves the granulator from the N_z-th or the last compartment. The particle flux term is discretized by using one of the finite volume schemes. In this paper, a high resolution scheme with Koren flux limiter function (KFL) is used to discretize the spatial domain. For this, the granulator is divided into N_z uniformly spaced compartments, and each compartment is assumed to be *perfectly mixed*. Integration of the particle flux term for N_z compartments gives

$$\frac{\partial}{\partial z}\left(\frac{dz}{dt} m_{i,z}\right) = w\frac{\partial}{\partial z}(m_{i,z}) = w\left[m_{i,z-\frac{1}{2}} - m_{i,z+\frac{1}{2}}\right], \tag{6}$$

where $\frac{dz}{dt} = w$ is the particle velocity along the granulator and is assumed to be constant inside the granulator. The approximation of the terms $m_{i,z\pm\frac{1}{2}}$ is then performed using a KFL scheme (Koren, 1993). The approximation of the terms $m_{i,z\pm\frac{1}{2}}$ using the KFL scheme is given by Eq. 7 and Eq. 8.

$$m_{i,z-\frac{1}{2}} \approx \frac{1}{\Delta z}\left\{\frac{M_{i,z-1}}{L_i} + \frac{1}{2}\phi\left(\theta_{i-\frac{1}{2}}\right) \times \left(\frac{M_{i,z-1}}{L_i^3} - \frac{M_{i,z-2}}{L_i^3}\right)\right\}, \tag{7}$$

$$m_{i,z+\frac{1}{2}} \approx \frac{1}{\Delta z}\left\{\frac{M_{i,z}}{L_i} + \frac{1}{2}\phi\left(\theta_{i-\frac{1}{2}}\right) \times \left(\frac{M_{i,z}}{L_i^3} - \frac{M_{i,z-1}}{L_i^3}\right)\right\}, \tag{8}$$

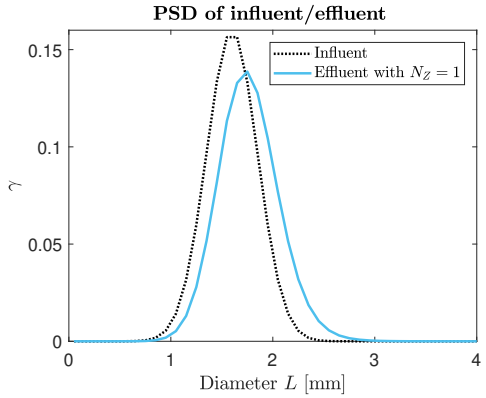

Figure 5. PSD of influent and effluent.

where, M_i is the total mass of the particle in the i^{th} class and $\Delta z = \frac{L_g}{N_z}$ is the length of the each section in the granulator (Figure 3). The limiter function ϕ in Eq. 7 and Eq. 8 is defined as

$$\phi(\theta) = \max\left[0, \min\left(2\theta, \min\left(\frac{1}{3} + \frac{2\theta}{3}, 2\right)\right)\right], \quad (9)$$

and parameter θ is defined as

$$\theta_{i-\frac{1}{2}} = \frac{\frac{M_{i,z}}{L_i^3} - \frac{M_{i,z-1}}{L_i^3} + \varepsilon}{\frac{M_{i,z-1}}{L_i^3} - \frac{M_{i,z-2}}{L_i^3} + \varepsilon}, \quad \theta_{i+\frac{1}{2}} = \frac{\frac{M_{i,z+1}}{L_i^3} - \frac{M_{i,z}}{L_i^3} + \varepsilon}{\frac{M_{i,z}}{L_i^3} - \frac{M_{i,z-1}}{L_i^3} + \varepsilon}. \quad (10)$$

The constant ε is a very small number to avoid division by zero, e.g. $\varepsilon = 10^{-8}$.

3 Application of PBE to granulation process in rotary drums

The model for the rotary drum granulator (continuous agglomeration process) includes binary agglomeration of the particles and is given as

$$\frac{\partial m(L,z,t)}{\partial t} = B(L,z,t) - D(L,z,t) - \frac{\partial}{\partial z}\left[\frac{dz}{dt} m(L,z,t)\right]. \quad (11)$$

To solve the model, the entire particle size range is divided into uniformly distributed classes. The particle flux term (the last term on the right hand side of Eq. 11) is treated in two different ways as described in detail in Section 2.2. The agglomeration terms (the first two terms on the right hand side of Eq. 11) are discretized using the cell average scheme (Kumar et al., 2006; Kumar, 2006) as well as Kumar et al.'s new finite volume scheme (Kumar et al., 2016).

The cell average (CA) scheme was introduced by Kumar (Kumar et al., 2006; Kumar, 2006) and it belongs to the sectional methods of discretization. In the CA scheme, at first the total birth of particles in each cell denoted is computed. Then the average volume of the newly formed particles in each cell is calculated. The next step in the CA scheme is to assign the total birth of particles appropriately to different cells depending on the position of the average volume of all newborn particles relative to the cell center volume. However, the CA scheme discussed in (Kumar et al., 2006; Kumar, 2006) is valid when the particle volume represents the internal coordinate. Thus, the volume based formulation of the CA scheme should be transformed into the diameter based formulation of the CA scheme. For this, the zeroth moment (total number of particles), and the third moment (total mass of particles) has been chosen to be conserved (compared to zeroth and first moments for volume based definition). Mathematical expressions of diameter based formulation for the CA scheme are given in (Vesjolaja et al., 2018).

Kumar et al.'s new finite volume scheme (Kumar et al., 2016) is based on the finite volume approach proposed by (Forestier and Mancini, 2012). Recently, new approach of solving PBE was proposed in (Kumar et al., 2016). This scheme is an accurate and efficient discretization method for agglomeration tern discretization. It has an improvement over the finite volume scheme proposed by (Forestier and Mancini, 2012) since it provides better solution of several moments in addition to the mass conservation property. Mathematical formulations are given in (Kumar et al., 2016).

Table 1. Parameters used for simulating granulation in spherodizers

Parameter	*Spherodizer*
Range of L [mm]	0-8
Number of cells	80
Grid type	linear
ρ [kg$\cdot$ m^{-3}]	1300
Length of granulator [m]	10
τ [min]	10
$\dot{m}_{\text{sl,i}}$ [kg$\cdot$ h^{-1}]	100
$X_{\text{sl,i}}$	0.05
Time step for RK4 [s]	20

In this paper, the agglomeration kernel (β) is defined using the Kapur agglomeration kernel model (Kapur, 1972) by taking $a = 2$ and $b = 1$. Using the diameter based formulation, the agglomeration kernel takes the form

$$\beta_{ik} = \left(\frac{6}{\pi}\right)^{\frac{2}{3}} \frac{1}{\rho} \beta_0 K_{ik}, \quad (12)$$

where the term $\left(\frac{6}{\pi}\right)^{\frac{2}{3}} \frac{1}{\rho}$ arises during the conversion from a number-based formulation to the mass-based formulation of PBEs, β_0 is the particle size independent part of the agglomeration kernel, and K_{ik} is the particle size dependent part of the agglomeration kernel as shown in Eq.13.

$$K_{ik} = \frac{(L_i + L_k)^2}{L_i L_k}, \quad (13)$$

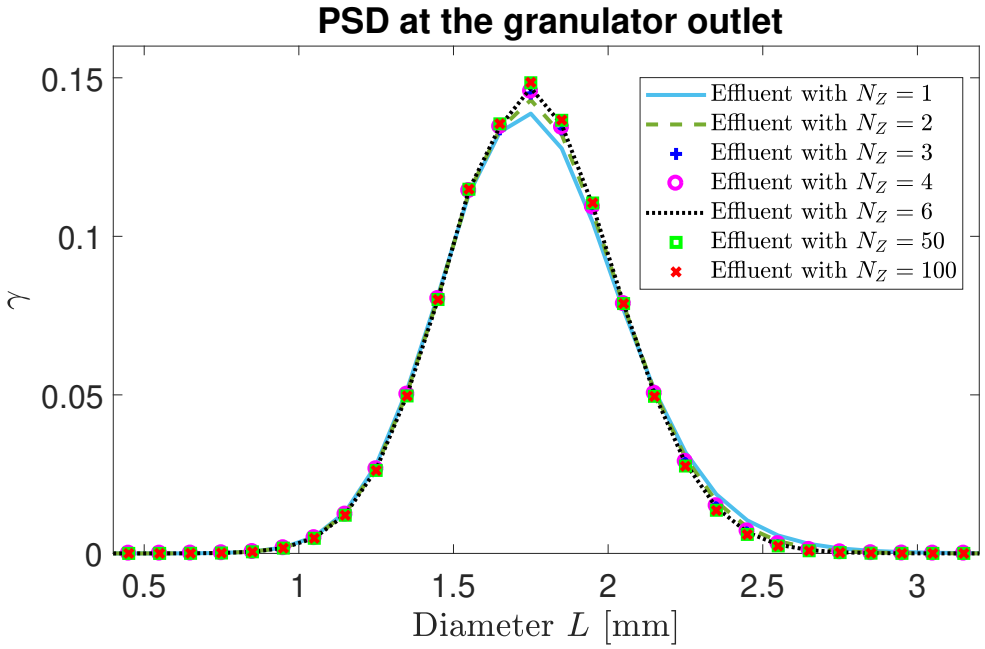

Figure 6. PSDs at the outlet of the spherodizer for different number of compartments.

4 Simulation Results and Discussion

4.1 Simulation Setup

The semi-discrete form (set of ODEs) of the PBEs obtained from particle class size and spatial discretizations are solved using a 4-th order Runge-Kutta method with fixed time step. Dynamic simulations are performed using MATLAB (MATLAB, 2017). The parameters used to simulate the application of PBE to the fertilizer granulation process in spherodizers and rotary drums are given in Table 1 and Table 2 respectively .

Table 2. Parameters used for simulating granulation in rotary drums.

Parameter	*Rotary drum*
Range of L [mm]	0-8
Number of cells	80
Grid type	linear
ρ [kg$\cdot$ m^{-3}]	1300
β_0 [s^{-1}]	$1.0 \cdot 10^{-11}$
Length of granulator [m]	6
τ [min]	6
$\dot{m}_{\mathrm{sl,i}}$ [kg$\cdot$ h^{-1}]	100
$X_{\mathrm{sl,i}}$	0.05
Time step for RK4 [s]	20

4.2 Simulation results for granulation in spherodizers

The granulation process in spherodizers is simulated for two simulation cases: Case I where the entire granulator is assumed 'perfectly mixed', and Case II where the entire granulator length is divided into uniformly sized compartments as described in Section 2.2.

Table 3. Comparison of the computational time (in seconds) with different numerical schemes for rotary drum simulations.

Numerical scheme	$\beta = \beta_0$	$\beta = \beta_{ik}$
CA with $N_z = 1$	3.3	6.0
CA with $N_z = 3$	9.0	17.0
NFV with $N_z = 1$	3.6	6.2
NFV with $N_z = 3$	9.1	17.3

The mass based formulation of the PBE with diameter representing the particle size, is used, and the spherodizer is a continuous process with influent and effluent. Table 1 lists the simulation settings and parameters values. Simulation results are presented by particle size distribution (PSD) plots in terms of particle diameter, as well as by particle median diameter d_{50}. The values of d_{50} are obtained from the cumulative mass distribution. Linear interpolation is used to extract d_{50} values that correspond to intercept for 50 % of cumulative mass.

Simulation results obtained for the application of the PBEs in spherodizers is depicted in Figure 4, Figure 5 and Figure 6. Figure 4 and Figure 5 shows the change in particle sizes that occurs during a continuous granulation process in the *perfectly mixed* spherodizer (solution of the PBE is found using KFL scheme). Clearly, the particles grow in size inside the granulator. As a result, d_{50} of the effluent is larger than d_{50} of the influent, Figure 4, and more of coarse-sized particles is produced,

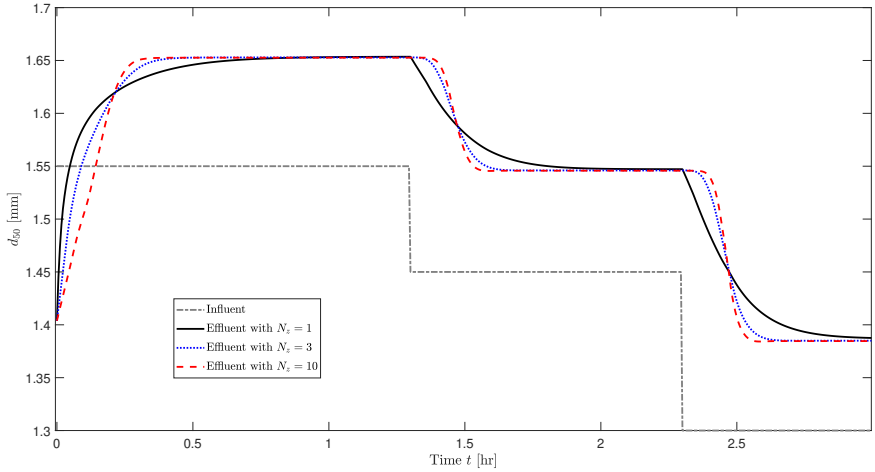

Figure 7. d_{50} at the outlet of the spherodizer for different number of compartments.

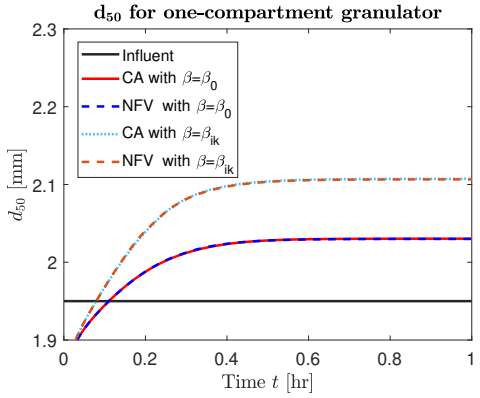

Figure 8. Simulation results for d_{50} with size-dependent and size-independent agglomeration kernels assuming *perfectly mixed* drum granulator.

Figure 5. Simulation results with the inclusion of spatial discretization of the granulator are depicted in Figure 6 and Figure 7. In Figure 6, PSDs of the effluent at the outlet of the granulator with different number of compartments (N_z) are compared. The PSD plot with $N_z = 50$ can be considered as a reference plot since no change in PSD is observed when increasing the number of compartments in the granulator (PSD plot with $N_z = 100$). Differences in PSDs appear mainly for the coarser particle fractions (with $L > 1.5$ mm), while for the finer particles (with $L < 1.5$ mm), the *perfectly mixed* granulator gives accurate enough results. Figure 7 shows d_{50} of the effluent as a step change in the influent is given. In a multi-compartment granulator a time delay is introduced as a step change of d_{50} in influent is given. Thus, inclusion of the spatial discretization could be important for development of a control-relevant dynamic model of the graulator. Based on Figure 6 and Figure 7, it can be concluded that diving the whole granulator space in 3 compartments could be sufficient to achieve a sufficiently accurate model compared to the *perfectly mixed* granulator ($N_z = 1$). The only disadvantage of discretizing the granulator in space is the increased computational time. As the value of N_z increases, i.e., as the number of compartments in the granulator increases, the computational time also increases. In particular, with a standard PC used for the simulation (i5 with 4 cores, 8 GB RAM and 2.1 GHz CPU), the computational time for one-compartment granulator was 0.5 s, and for the three-compartment granulator was 0.9 s (about 2 times more).

4.3 Simulation results for granulation in rotary drums

The granulation process in drum granulators is simulated using the CA scheme, as well as the NFV scheme. Similar to the spherodizers, the simulations have been performed for a multi-compartment drum granulator model and also with the *perfectly mixed* assumption. The mass based formulation of the PBE with particle diameter representing the size, is used to assess the PSD. The simulation results are also compared for a size-independent ($\beta = \beta_0$) and a size-dependent ($\beta = \beta_{ik}$) agglomeration kernel.

With the *perfectly mixed* assumption, i.e., for $N_z = 1$, the simulation results are depicted in Figure 8. As expected, the CA scheme and the NFV scheme produce similar results (d_{50} of the effluent) for both the size-independent and the size-dependent agglomeration kernels. Due to binary agglomeration, the particles grow in size. However, with the size-dependent agglomeration kernel, the d_{50} of the effluent is higher than with the size-independent constant kernel.

Simulation results for the multi-compartment drum granulator model are shown in Figure 9. Figure 9 compares the PSD of the influent, as well as PSDs of the effluents that correspond to each of the compartments of the granulator. Clearly, particles in the first compartment are smaller in size compared to the second and third compartments of the granulator. Particles increase in their sizes

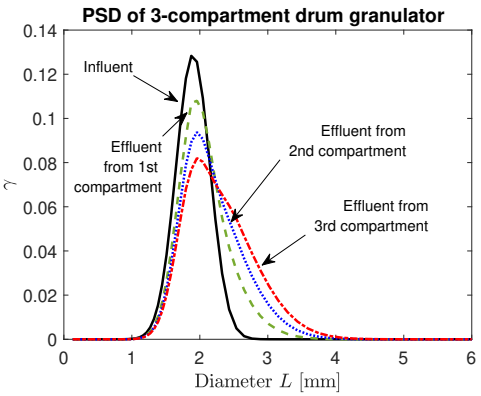

Figure 9. PSD for influent/effluent in 3-compartment drum granulator with the CA scheme.

as they are transported along the granulator, and as a result, the coarser fractions of the particles increase while their finer fractions decrease. The computational time is also compared for different choices of N_z as listed in Table 3. As expected, the computational time needed for solving the model increases with increasing the number of compartments in the drum granulator. This observation is valid with both the CA and the NFV schemes used to solve the model, and for both types of agglomeration kernels. However, inclusion of the size-dependent agglomeration kernel increase the computational time significantly: it takes almost twice the time to obtain the solution with size-dependent agglomeration kernel ($\beta = \beta_{ik}$) compared to the size-independent kernel $\beta = \beta_0$.

5 Conclusions

In this paper, the population balance equations for the spherodizer and the rotary drum granulator were developed. To account for property inhomogeneity in the granulators, multi-compartment models of the granulators were also developed. The simulation results showed that the discretization of the external coordinate (axial length of the granulator) in the model, introduces a transport (time) delay from the inlet of the granulator to its outlet. Inclusion of the correct transport delay is important for control studies. However, the ability of the model to capture transport delay inside the granulator comes with the cost of increased computational time. Two different discretization schemes, namely Kumar's new finite volume scheme and the cell average scheme showed similar simulation results in terms of the model solution accuracy and computational time. Model solution was obtained relatively fast for both simulation scenarios: with the constant agglomeration kernel and with the size-dependent agglomeration kernel. Thus, the developed models and model solution techniquies can be used for further control-relevant studies.

6 Acknowledgment

The economic support from The Research Council of Norway and Yara Technology Centre through project no. 269507/O20 'Exploiting multi-scale simulation and control in developing next generation high efficiency fertilizer technologies (HEFTY)' is gratefully acknowledged.

References

I.T. Cameron, F.Y. Wang, C.D. Immanuel, and F. Stepanek. Process systems modelling and applications in granulation: A review. *Chemical Engineering Science*, 60(14):3723–3750, 2005.

L. Forestier and S. Mancini. A finite volume preserving scheme on nonuniform meshes and for multidimensional coalescence. *SIAM Journal of Scientific Computing*, 34(6), 2012. doi:10.1137/110847998.

C. Herce, A. Gil, M. Gil, and C. Cortés. A cape-taguchi combined method to optimize a npk fertilizer plant including population balance modeling of granulation-drying rotary drum reactor. In *Computer Aided Chemical Engineering*, volume 40, pages 49–54. Elsevier, 2017.

PC Kapur. Kinetics of granulation by non-random coalescence mechanism. *Chemical Engineering Science*, 27(10):1863–1869, 1972.

B. Koren. A robust upwind discretization method for advection, diffusion and source terms. In C. B. Vreugdenhil and B. Koren, editors, *Numerical Methods for Advection-Diffusion Problems, Notes on Numerical Fluid Mechanics*, pages 117–138. 1993.

J. Kumar. *Numerical approximations of population balance equations in particulate systems*. PhD thesis, Otto-von-Guericke-Universität Magdeburg, Universitätsbibliothek, 2006.

J. Kumar, M. Peglow, G. Warnecke, S. Heinrich, and L. Mörl. Improved accuracy and convergence of discretized population balance for aggregation: The cell average technique. *Chemical Engineering Science*, 61(10):3327–3342, 2006.

J. Kumar, G. Kaur, and E. Tsotsas. An accurate and efficient discrete formulation of aggregation population balance equation. *Kinetic & Related Models*, 9(2), 2016.

J. Litster and B. Ennis. *The science and engineering of granulation processes*, volume 15. Springer Science & Business Media, 2004.

MATLAB. 2017a. The MathWorks, Inc., Natick, Massachusetts, United States., 2017.

R. Ramachandran, C.D. Immanuel, F. Stepanek, J.D. Litster, and F.J. Doyle III. A mechanistic model for breakage in population balances of granulation: Theoretical kernel development and experimental validation. *Chemical Engineering Research and Design*, 87(4):598–614, 2009.

D. Ramkrishna. *Population balances: Theory and applications to particulate systems in engineering*. Academic press, 2000.

G. Valiulis and R. Simutis. Particle growth modelling and simulation in drum granulator-dryer. *Information Technology and Control*, 38(2), 2009.

L. Vesjolaja, B. Glemmestad, and B. Lie. Population balance modelling for fertilizer granulation process. *Proceedings of The 59th Conference on Simulation and Modelling (SIMS 59), 26-28 September 2018, Oslo Metropolitan University, Norway*, 2018.

F.Y. Wang, X.Y. Ge, N. Balliu, and I.T. Cameron. Optimal control and operation of drum granulation processes. *Chemical Engineering Science*, 61(1):257–267, 2006.